J Nanostruct 10(4): 779-792, Autumn 2020

RESEARCH PAPER

Production of Silica-alginate-nanocellulose Composite Beads with Cinnamon Essential Oil for Antimicrobial Sachet

Farah Fahma[1,*], RM Muhammad Nur Fauzan[1], Titi Candra Sunarti[1], Sugiarto[1], Abdul Halim[2], Kuan-Hsuan Lin[2], Donghao Hu[2], Toshiharu Enomae[2]

[1] *Department of Agroindustrial Technology, Faculty of Agricultural Engineering and Technology, IPB University (Bogor Agricultural University), Gedung Fateta, Kampus IPB Dramaga, Bogor 16680, Indonesia*

[2] *Faculty of Life and Environmental Sciences, University of Tsukuba, Tsukuba, Ibaraki 305-8572, Japan*

ARTICLE INFO

Article History:
Received 07 June 2020
Accepted 18 August 2020
Published 01 December 2020

Keywords:
Antimicrobial sachet
Cinnamon essential oil
Composite beads
Food safety
Nanocellulose

ABSTRACT

The production of antimicrobial sachet from silica-alginate-nanocellulose composite beads as carrier materials with the addition of nanocellulose (0, 1, 3, 5%) as nanofiller and cinnamon essential oil (CEO) as antimicrobial agent was investigated. The nanocellulose was isolated from oil palm empty fruit bunches by mechanical treatment using a combination of ultrafine grinding and ultrasonication. The produced composite beads were observed by scanning electron microscopy (SEM), Fourier transform infrared (FTIR) spectroscopy, thermogravimetric analysis (TGA), and x-ray diffraction (XRD) analysis. The produced composite beads with 5% nanocellulose (BDCN5) was more compact and spherical than others. Meanwhile, the produced antimicrobial sachets were performed with release characteristic and antimicrobial tests. The antimicrobial sachet with the addition of nanocellulose showed the cinnamon essential oil was significantly released from beads for 60 min and had a high inhibitory effect. Almost all microorganisms tested by BDCN5 showed a high inhibitory effect, 5.43% for inhibiting *Escherichia coli*, 5.19% for *Salmonella* sp, 3.36% for *Aspergillus* sp, and 8.72% for *Staphylococcus aureus*.

How to cite this article
Fahma F, Nur Fauzan RMM, Candra Sunarti T, Sugiarto, Halim A, Lin2, Donghao Hu KH, Enomae T. Production of Silica-alginate-nanocellulose Composite Beads with Cinnamon Essential Oil for Antimicrobial Sachet. J Nanostruct, 2020; 10(4): 779-792. DOI: 10.22052/JNS.2020.04.011

INTRODUCTION

Food safety is an important requirement that must be met before food is consumed by people. Food damaged by microorganisms (yeast, fungi, and bacteria) can be dangerous for health. Antimicrobial packaging is one of the innovative technological concepts of active packaging that can increase food safety and extend the shelf life of products by inhibiting undesirable microorganisms [1].

Antimicrobial agents, incorporation methods, resistance of microorganisms, controlled release, release mechanism, chemical nature of foods and antimicrobials, storage and distribution conditions, and antimicrobial packaging materials are some factors that can influence the effectiveness of antimicrobial packaging [2]. The antimicrobial function can be achieved by using an antimicrobial polymer that meets conventional packaging requirements or adding antimicrobial agents in the packaging system. The latter includes adding antimicrobial agents into the polymer matrix, coating it onto the packaging internal-surface, or immobilizing it in sachets [1, 2].

There are two types of antimicrobial sachet based on how to produce them. First type is sachets that produce antimicrobial compounds in situ and release it and the second is sachets that carry and release antimicrobials. The principle of

* *Corresponding Author Email: farah_fahma@apps.ipb.ac.id*

antimicrobial sachets involves the adsorption of antimicrobial compounds into the carrier matrix which then allows controlled release into an enclosed packaging system. The type of materials/ matrix used to carry volatile compounds affects the loading and release capacities of antimicrobial sachets [3].

Silica powder can act as the carrier of ethanol and carry its vapor through the sachet into the headspace of packaging [4]. Seo et al. [5] prepared antimicrobial sachet by encapsulating allyl isothiocyanate with alginate beads. Calcium alginate beads and silica (SiO_2) can be used as a carrier material for antimicrobial compounds for the production of sachets [3].

Cellulose is an abundant natural polymer in earth. Oil Palm Empty Fruit Bunches (OPEFBs) is biomass produced by Crude Palm Oil (CPO) industry. According to Richana et al [6], OPEFB has high enough cellulose content (41.3-45%), hemicellulose (25.3-33.8%), and lignin (27.6-32.5%). Cellulose in nano-size or nanocellulose is a new class of cellulose materials. In a previous study, we succeeded in producing nanocellulose using mechanical treatment, a combination of ultrafine grinding and ultrasonication [7]. Due to high specific surface area, high crystallinity, and the ability to form hydrogen bonds resulting in strong network, nanocellulose has an excellent barrier property for molecules to pass through it [8,9].

Cinnamon (*Cinnamomum zeylanicum*) essential oil has good antimicrobial activity against some microorganisms [10]. Cinnamaldehyde was identified as the most active antimicrobial component in the cinnamon essential oil. Cinnamon is one of the potential agricultural commodities in Indonesia and is one of the export commodities [11].

Based on the description above, this study aims to produce antimicrobial sachet with the addition of nanocellulose to slow down the release of antimicrobial compounds from composite beads and it was able to inhibit microbial activities.

MATERIALS AND METHODS

Materials

OPEFBs as raw material for producing nanocellulose was from PT Inti Indosawit Subur, Riau, Indonesia. Cinnamon essential oil (CEO) was from CV Pavettia Atsiri (Subang, West Java, Indonesia). The chemicals used were sodium alginate supplied from HiMedia Laboratories Pvt. Ltd., India (CAS-No: 9005-38-3), and calcium chloride dihydrate ($CaCl_2$* $2H_2O$) with molecular weight of 147.02 g/mol made in Germany (CAS-No: 10035-04-8), silica gel 60 (Merck), nutrient broth (NB), potato dextrose broth (PDB), nutrient agar (NA), potato dextrose agar (PDA), NaOH (Merck), Hydrogen peroxide (H_2O_2, Merck), and other chemical materials for analysis.

Isolation of cellulose

OPEFBs were cut into small pieces approximately 0.5 - 1 cm, washed, and boiled in water for 1 h to remove impurities, and dried in an oven at 55 °C for 24 h. Then, about 50 g of dried fibers of OPEFBs were immersed in 1000 mL solution of NaOH 10% (w/v), heated at 95 °C for 1 h and subsequently, washed with distilled water to neutral pH. The delignified fibers were bleached using 30% H_2O_2 (w/v) at 95-100 °C for 1.5 h and subsequently, rinsed with distilled water. Then, the fibers were bleached again using alkali peroxide. Alkali peroxide was obtained by mixing 200 ml solution of 30% H_2O_2 (w/v) and 100 ml solution of 10% NaOH (w/v). Furthermore, treated fibers were soaked in an alkali peroxide solution and stirred until the color became white and rinsed by water to neutral pH. The obtained cellulose was stored in refrigerator for the preparation of nanocellulose.

Preparation of nanocellulose

The cellulose was diluted with distilled water to a concentration of 2% w/w solid content. The suspension formed was passed through an ultrafine grinder (Matsuko Corp, Japan) several times at 1500 rpm. Hereinafter, the suspension was ultrasonicated with 80% amplitude for 60 min to obtain nanocellulose.

Production of silica-alginate-nanocellulose composite

The method used for the production of composite beads was dropping off the mixture of sodium alginate, silica, and nanocellulose into the 10% $CaCl_2$ solution (w/v). The formulation to produce silica-alginate-nanocellulose composite beads is shown in Table 1.

Firstly, nanocellulose and distilled water were stirred until it became homogeneous suspension using a magnetic stirrer at room temperature. Then, silica was added into the suspension and stirred for 30 minutes. After that, sodium alginate was added into the suspension and stirred

Table 1. The formulation of silica-alginate-nanocellulose composite beads

Sample	Silica (%)	Sodium Alginate (%)	Water (%)	Nanocellulose (%)
BDNC0	1	2	97	0
BDNC1	1	2	96	1
BDNC3	1	2	94	3
BDNC5	1	2	92	5

BDNC: Silica-Alginate-Nanocellulose Composite Beads, NC: Nanocellullose

until becoming a homogeneous solution. Then, cinnamon essential oil 3% (w/w) and tween 80 3% (w/w) were added into the solution and stirred again. The obtained solution was dropped off into the $CaCl_2$ solution (10%, w/v) using syringe 21G to produce composite beads. Subsequently, the produced composite beads were rinsed with distilled water.

Antimicrobial sachet production

The produced composite beads (0.5 g) were packaged on a sealed filter paper with a size of 2.5 cm x 3 cm. Then, the produced antimicrobial sachet was analyzed by a release characteristic and antimicrobial test.

Scanning electron microscope (SEM) observation

The morphology of obtained nanocellulose and produced silica-alginate-nanocellulose composite beads was analyzed by SEM (SU8020 Hitachi) with an accelerating voltage of 1 kV. The diameter size of nanocellulose was measured using imageJ software.

Transmission electron microscopy (TEM) observation

The morphology of nanocellulose was also analyzed by TEM (H-7650 Hitachi). The Observation was performed by an accelerating voltage of 80 kV.

Fourier transform infra-red (FTIR) spectroscopy

FTIR spectra of nanocellulose and silica-alginate-nanocellulose composite beads were recorded in an FTIR-6100 Jasco to examine the changes in functional groups induced by various treatments. The FTIR analysis was performed within a range of 500-4000 cm^{-1}.

X-ray diffraction (XRD) analysis

XRD measurement was performed to determine the crystalline index of nanocellulose and silica-alginate-nanocellulose composite beads. The measurement was carried out using a Rigaku RINT 2000 for nanocellulose and x-ray diffractometer D8 Advance/TSM with radiation of Kα Cu (λ = 1.54060) for silica-alginate-nanocellulose composite beads. The crystallinity index (CI) was calculated from diffraction profiles as the ratio of the area under the crystalline diffraction peaks to the total area under the curve. It was calculated by using Segal's method using the following equation:

$$CI(\%) = \frac{I_{crystalline}}{I_{crystalline} + I_{amorphous}}$$

Thermo-gravimetric analysis (TGA)

The thermal stability of nanocellulose and its composite beads were analyzed using a Thermo-Gravimetric Analyzer (TG/DTA 7300 Exstar). Approximately 5-10 mg samples were burned, nanocellulose from 50-400 °C and for silica-alginate-nanocellulose composite beads from 50-800 °C under an argon atmosphere at a heating rate 20 °C/min.

Release characteristic of cinnamon essential oil (CEO) from composite beads

Antimicrobial sachets were placed in a desiccator at RH 80%. The release characteristic of CEO from the composite beads were analyzed for up to 6 days. The remaining CEO in the composite beads was calculated by:

Release (%) = $(CEO_0\text{-}CEO_t/CEO_0) \times 100$

where CEO_0 was the amount of CEO initially entrapped in the composite beads and CEO_t was the amount of CEO remaining in the beads at a given time t.

Antimicrobial test (total plate count method)

The performance of antimicrobial sachet

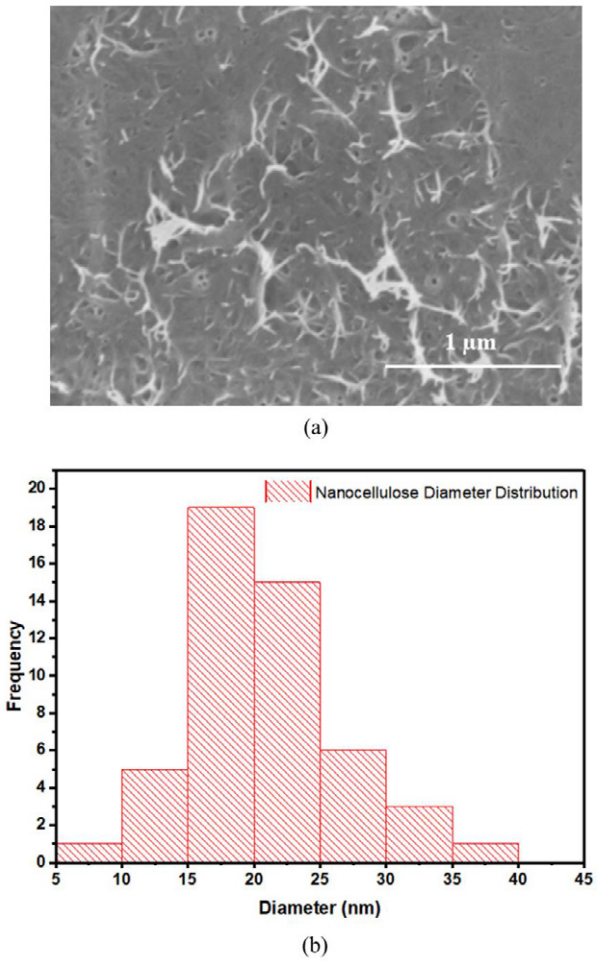

Fig. 1. (a) SEM image of the obtained nanocellulose and (b) frequency of nanocellulose diameter distribution.

was observed by calculating the inhibition of microorganism growth due to the influence of antimicrobial sachet. The microorganism used were *Escherichia coli*, *Salmonella* sp, *Staphylococcus aureus*, and *Aspergillus* sp. One day before the test, the culture of microorganisms was grown in the nutrient broth media for bacteria and potato dextrose broth for mold. Petri dishes, pipettes, and test tubes used for this test were sterilized in an autoclave at 121 °C for 15 min. The agar media for bacteria and mold were also sterilized in an autoclave at 121 °C for 15 min. The diluent solution was prepared by dissolving 1.7 g NaCl in 200 ml of distilled water which was sterilized in an autoclave at 121°C for 15 min. A sample (1 ml) of *each culture* was *taken,* then put the solution into test tube containing 9 ml of a sterile diluted solution to obtain 10^{-2} dilution and so on until obtained dilution 10^{-5}. From each tube, the diluted solution was taken 0.1 ml, then put into a sterilized petri dish. Then, each petri dish was poured out with agar media, stirred it well and let it solidify. After that, the petri dish was turned over and antimicrobial sachet put in each petri dish and taped on another side of the dish and wrapped with plastic wrap. Then, petri dishes were kept in an incubator for 24 h. Formed colonies were counted using a Quebec colony counter.

RESULTS AND DISCUSSION

Nanocellulose morphology

Fig. 1 and Fig. 2 show SEM and TEM images of nanocellulose, respectively. Based on Fig. 1, most of nanocellulose diameters was in nano-size and the average of nanocellulose diameter obtained was 19.55 ± 0.40 nm. The length of nanocellulose could not be measured because the

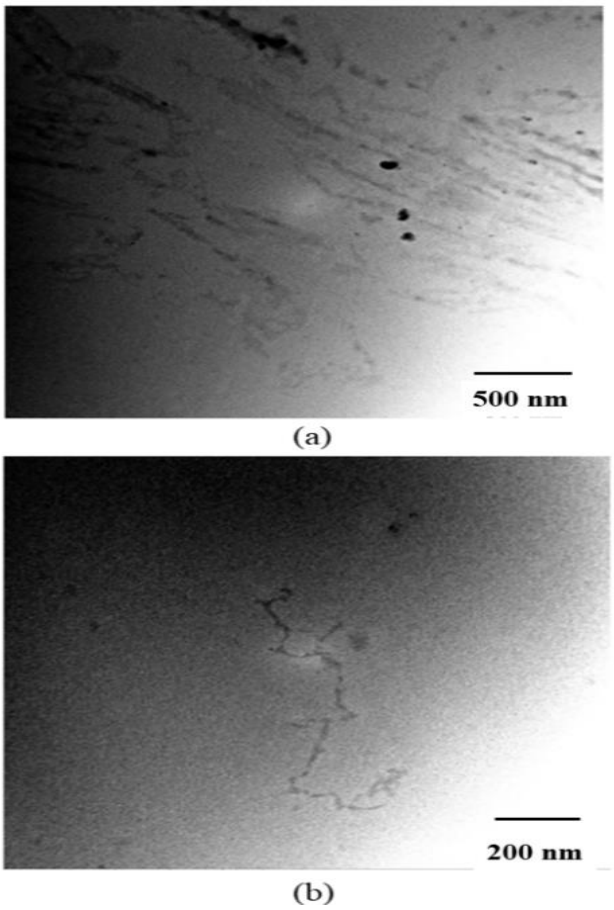

Fig. 2. TEM Image of the obtained nanocellulose.

end of nanocellulose was difficult to find in the SEM image. The TEM result shows that the length of nanocellulose was estimated in the micrometer size. This result was appropriate with the study conducted by Fahma et al. [12] that the obtained nanocellulose had the length in the range of 100 nm - 2 µm.-

In this study we isolated nanocellulose using a combination of ultrafine grinding and ultrasonication. The cellulose suspension was passed through between a static and a rotating grindstones 37 times at 1500 rpm. According to Mishra et al. [13] the mechanism of ultrafine grinding is shearing forces generated by the grinding stones breaks down the cell wall structure consisting of nanofibers in a multi-layered structure and hydrogen bonds. As a result, nanosized fibers were individualized from the pulp. Ultrasonication was carried out to produce homogeneous nano-size cellulose due to cavitation effect in nanocellulose suspension so that the formation of bubbles produced high ultrasonic energy and make particles more homogeneous [14]. Iwamoto et al. [15] succeeded to prepare uniformly nano-sized fibrillation of pulp fibers by only ultrafine grinder without high pressure homogenizer. Meanwhile, this present result indicates that it is not possible to produce nanofibers uniformly without ultrasonication. Fig. 1 and 2 indicate that by 37 passes through the ultrafine grinder and ultrasonication the fibrillation of cellulose fibers was completely accomplished.

Chemical compound analysis of nanocellulose

Fig. 3 shows the FTIR spectrum of the obtained nanocellulose from OPEFBs. Cellulose is composed of three functional groups, namely O-H, C-H, and C-O groups. Table 2 shows the identified lignin still exist in nanocellulose even a little [16]. FTIR vibration observed in the obtained nanocellulose.

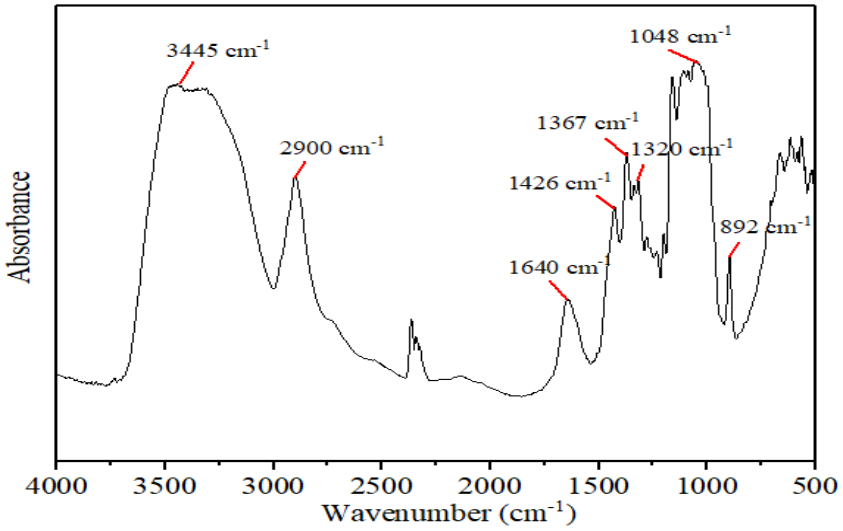

Fig. 3. FTIR spectrum of the obtained nanocellulose.

Table 2. FTIR vibrations observed in the obtained nanocellulose

Wavenumber (cm^{-1})	Components
3445	O-H
2900	C-H Aliphatic
1640	Adsorbed water Fiber O-H
1320-1426	C=C (lignin), C-H deformation of cellulose and lignin
1048	C-O streching
892	C-H Aromatic

The FTIR spectrum of nanocellulose showed that a peak at 3445 cm^{-1} attributed to O-H groups from cellulose. The C-H group was found at 2900 cm^{-1} which identified the aliphatic compound. The C-O stretching at 1048 cm^{-1} was corresponded to the phenol compound and the band at 1320-1426 cm^{-1} was related to the C=C group.

According to Lojewska et al. [17], a peak at 1640 cm^{-1} was an O-H bending of absorbed water. However, the water adsorbed in the cellulose molecules is difficult to extract due to the cellulose-water interaction [18]. Lignin might still exist at 1426 cm^{-1}. From the FTIR profile, lignin was reduced and hemicellulose was successfully removed because hemicellulose did not appear at peak around 1700 cm^{-1}. Therefore, with delignification and bleaching treatment, it was effective to reduce lignin and remove hemicellulose to prepare nanocellulose.

Crystallinity of nanocellulose

Fig. 4 shows the XRD profile of the obtained nanocellulose. The main diffraction peak was at around 22.1° and the low-intensity peaks were around 14.7° and 16.3°. The XRD profile was typical of cellulose I according to Arnata et al. [19]. The crystallinity of nanocellulose obtained was 61.2%. Generally, the crystallinity of nanocellulose is higher than its cellulose fibers [20,21]. Under certain conditions, crystallinity of nanocellulose isolated by mechanical treatment is higher than that of isolated by chemical treatment. With long hydrolysis time and high acid concentration in chemical treatment, the crystalline regions of cellulose will be destroyed causing the crystallinity of nanocellulose to be low [12,20,21].

Characterization of silica-alginate-nanocellulose composite beads

Morphology

According to Waldman et al., in order to make beads sodium alginate needs to contact with divalent ions, such as calcium (Ca^{2+}). When sodium alginate solution is dropped off into a solution of calcium chloride, a bead forms instantly as the

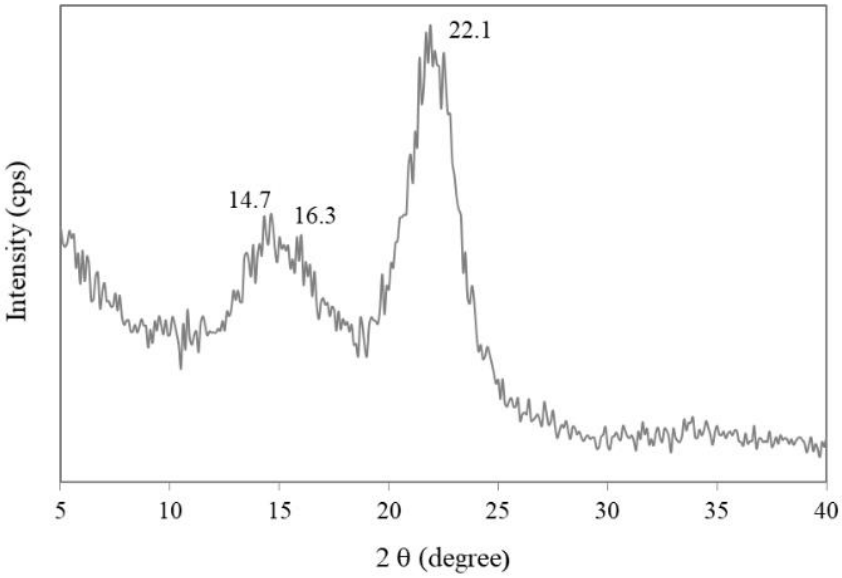

Fig. 4. XRD profile of the obtained nanocellulose.

Fig. 5. Produced composite beads.

sodium ions (Na^+) are exchanged with calcium ions (Ca^{2+}) and the polymers become cross-linked [22]. Fig. 5 shows the obtained composite beads. Fig. 6 shows the SEM images of the produced composite beads with the addition of nanocellulose. The produced composite beads are relatively spherical and porous, with diameter size of about 0.3 cm.

The present result indicates that calcium ions in the calcium chloride solution cross-linked the alginate mixed with silica, attaching each other at many points. The cross-linking produced solid composite beads. Longer immersion in $CaCl_2$ causes more calcium ions to move into the beads, resulting in more cross-linking and firmer textures [23].

Based on the SEM images, with increasing nanocellulose content, the morphology of composite beads become more compact. The composite bead with 5% nanocellulose had a more compact structure and spherical shape than others.

Chemical compounds FTIR analysis of composites

Fig. 7 shows the FTIR profiles of the produced composite beads and Table 3 shows the FTIR vibrations observed in the produced

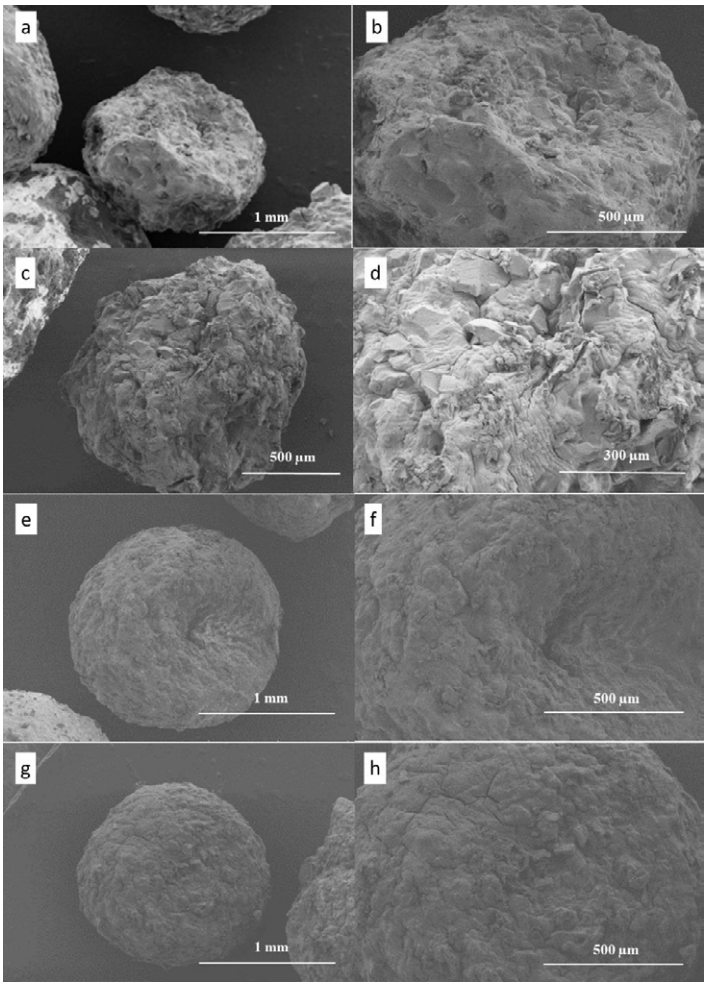

Fig. 6. SEM images of the produced composite beads with addition of nanocellulose: 0% (a, b), 1% (c, d), 3% (e, f), and 5% (g, h).

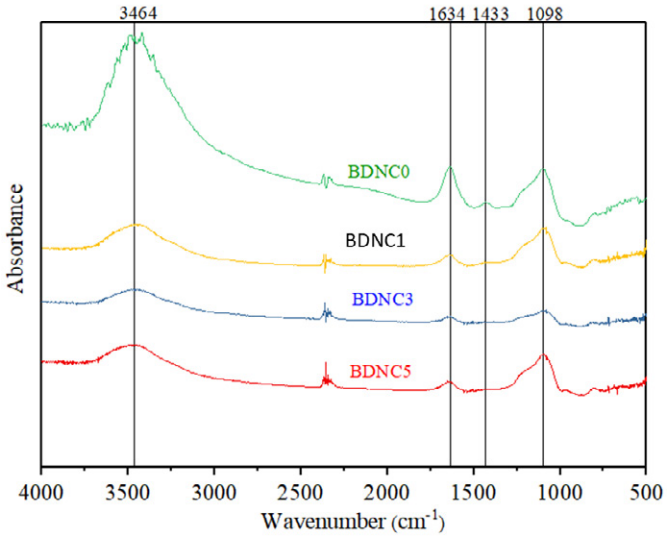

Fig. 7. FTIR profile of produced composite beads.

Table 3. FTIR vibrations observed in the produced composite beads

Wavenumber (cm^{-1})	Components
3464	O-H
1634 and 1433	Adsorbed water Fiber O-H
1098	Si-O

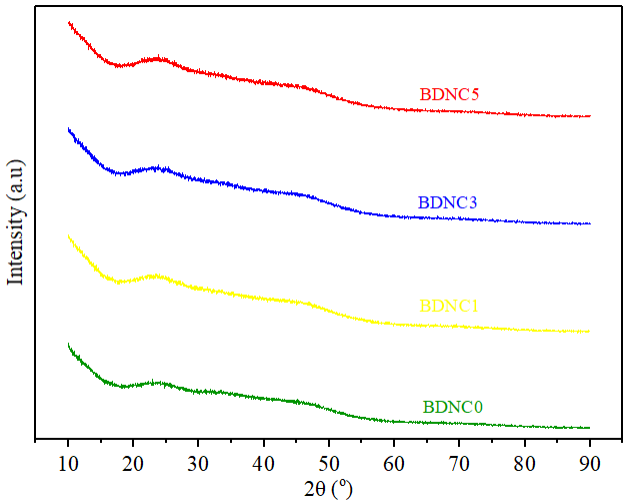

Fig. 8. XRD profile of produced composite beads.

composite beads. The wavenumber at 3464 cm^{-1} corresponded to O-H groups. The peaks at 1634 cm^{-1} and 1433 cm^{-1} were an O-H bending [16]. Wavenumber at 1098 cm^{-1} (in the range of 830-1110 cm^{-1}) was corresponding to Si-O which was identified as silica in composite [24]. Based on Fig. 7, with the addition of nanocellulose, the intensity of the OH group decreased. This might be caused by the binding between the OH group of nanocellulose and the OH group of alginate and silica. The decrease of intensity of OH group can be seen at 3464 cm^{-1} in the samples of BDNC1, BDNC3, and BDNC5 but the difference was not significant. It seems that the nanocellulose addition up to 5% still did not make a difference in the FTIR spectra.

Crystallinity of composite beads

Fig. 8 shows the XRD profiles of the produced composite beads. The addition of nanocellulose did not give different profiles with a neat silica-alginate composite bead. Silica and alginate are amorphous materials so that the composite tends to be amorphous [25]. The crystallinity of composite polymers is influenced by the nucleation and confinement by fillers in the matrices [26].

Thermal stability

Thermogravimetric analysis (TGA) is an analytical technique used to determine the thermal stability of a material and its fraction of volatile components by monitoring the change in weight due to a sample being heated at a constant rate [27]. Fig. 9 shows TGA and DTG profiles of obtained nanocellulose and produced composite beads. In nanocellulose thermal degradation, two main stages could be observed. The first stage occurred in the range from 50 to 150 °C relating to the loss of water from the nanofibers sample. The second stage was observed to start at around 250 °C, regarding to the degradation and decomposition of the chemical structure of cellulose (glycosidic bonds) [28]. Meanwhile, the composite beads started to degrade at around 196 - 205 °C. For composite beads with nanocellulose concentrations of 0, 1, 3, and 5%, the profiles of decomposition steps were similar for each other. Their profiles were very close to the degradation of sodium alginate which has two degradation

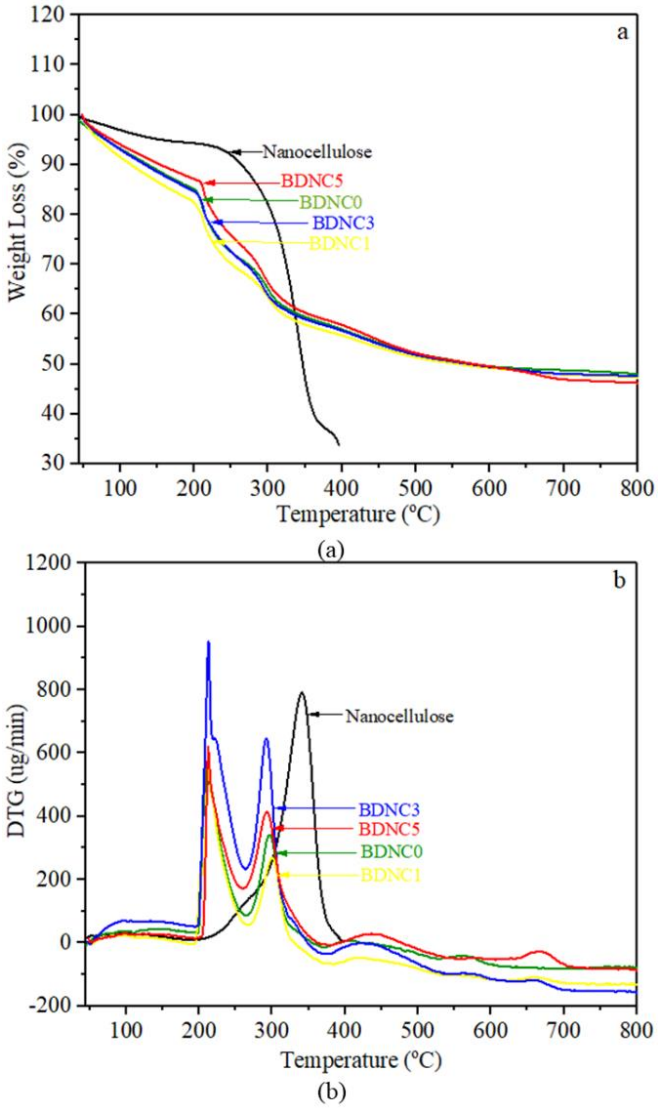

Fig. 9. TGA (a) and DTG (b) profiles of obtained nanocellulose and produced composite beads.

steps at 200 - 300 °C and 500 - 600 °C [29]. As also seen from the DTG curves, the addition of 1% of nanocellulose resulted in the decrement of composite beads maximum rate of weight loss. However, in further addition, their maximum rate of weight loss increased, which might be happened due to the degradation and decomposition of nanocellulose.

With 5% nanocellulose content the thermal stability of the composite beads shifted to higher temperatures, indicating that 5% nanocellulose is able to delay the thermal degradation of the polymer matrix. It is strongly influenced by the intermolecular bonding between nanocellulose and silica-alginate matrix. Therefore, well-dispersed nanocellulose and a good interfacial adhesion between nanocellulose and polymer matrix are needed to increase the thermal stability of their composite [26].

Table 4 shows the residual weight of nanocellulose and composite beads. A total of 33.67% of the nanocellulose residual weight was remained at a 400°C. The weight fraction of nanocellulose that still existing after heating above 400◦ C is representative of the char residue of the fibers [30]. Meanwhile, at 800 °C composite beads with the addition of nanocellulose 0, 1, and 3% had almost the same amount of residual weight which consist mostly

Table 4. Residual weight of nanocellulose and composite beads

Sample	Residual mass (%) at 800 °C
Nanocellulose*	33.67
BDNC0	47.85
BDNC1	47.25
BDNC3	47.48
BDNC5	46.12

*residual weight of nanocellulose was analyzed at 400 °C.

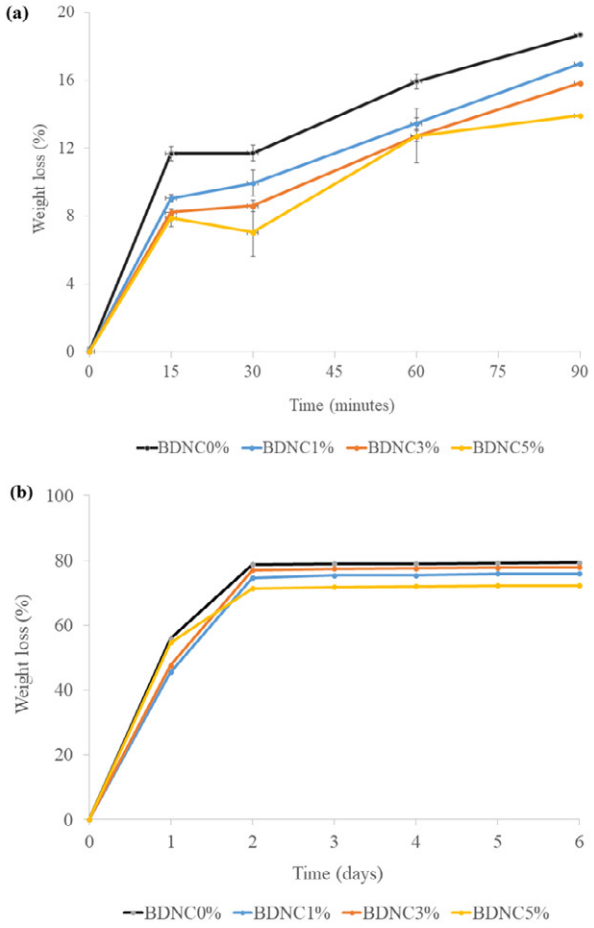

Fig. 10. Percentage of cinnamon essential oil released from produced composite beads into the atmosphere. Beads were stored in atmosphere at 80% RH up to (a) 90 min and (b) 6 days.

sodium carbonate residue [29]. Composite bead with 5% nanocellulose had residual weight which was slightly higher than the others.

Performance of antimicrobial sachet

Release characteristic test

A release test was performed to determine the release of CEO from composite beads. Release characteristics of CEO from composite beads were affected by time. This is supported by Seo et al. that the release characteristics of volatile compounds from antimicrobial sachets are affected by temperature, RH, and incubation time [5].

Fig. 10 shows the percentage of CEO released from composite beads at 80 % RH up to 90 min and

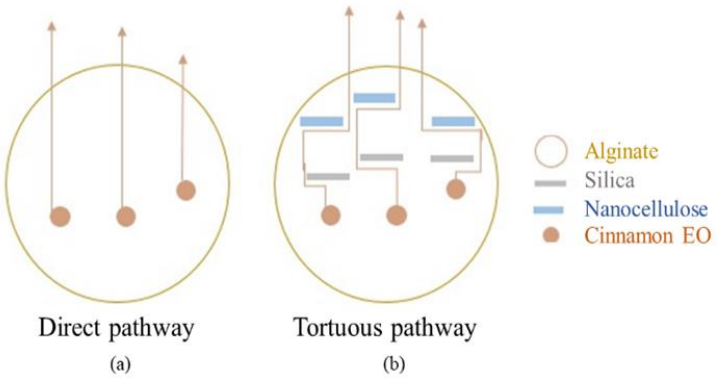

Fig. 11. The mechanism of release of cinnamon essential oil from composite beads.

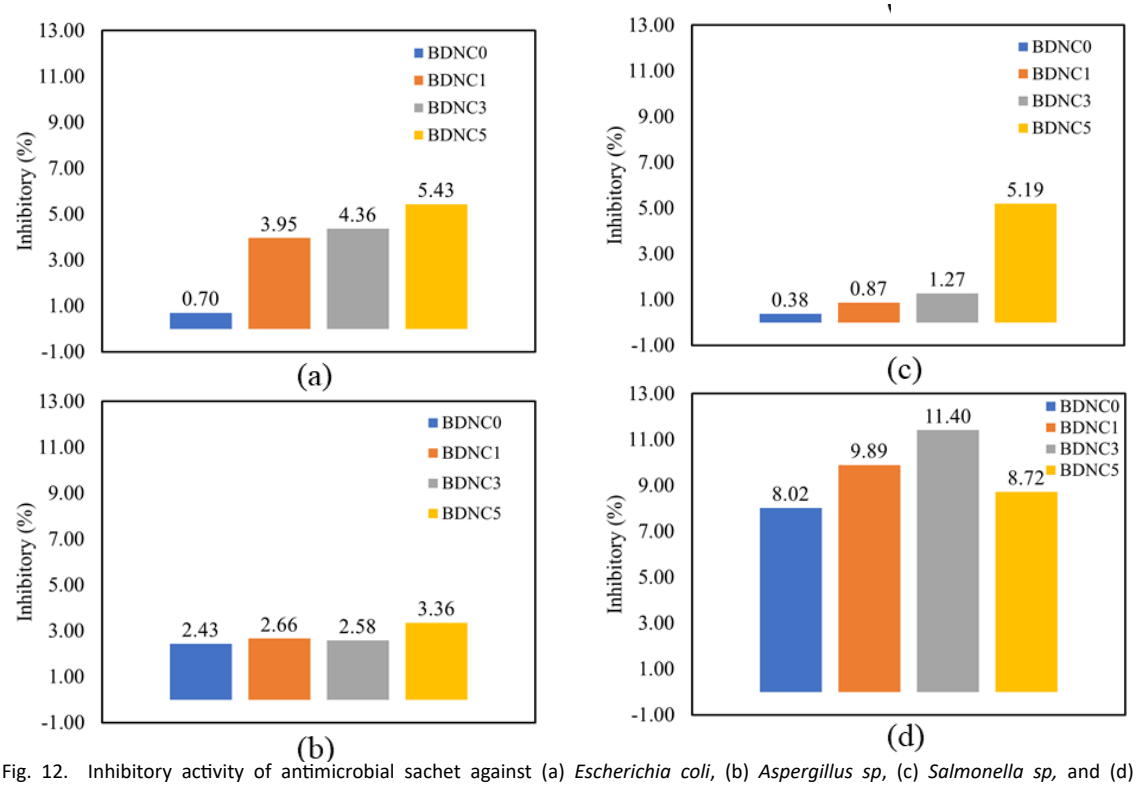

Fig. 12. Inhibitory activity of antimicrobial sachet against (a) *Escherichia coli*, (b) *Aspergillus sp*, (c) *Salmonella sp,* and (d) *Staphylococcus aureus.*

6 days. In the first 15 min, the CEO started to release from composite beads. CEO was significantly released from composite beads within 60 min and rapidly released from composite beads into the atmosphere within 2 days. Around 71.3-78.7% of the CEO was released from the composite beads after 2 days.

From this test, we could know that composite beads with 5% nanocellulose (BDNC5%) had a good ability to slow down the release of the CEO compared to the other composite beads. According to Lani et al., the presence of nanocellulose affects the diffusion pathway from a direct path to a tortuous path which leads to slow down the release of the CEO from composite beads [31]. Fig. 11 shows the mechanism of release of the CEO from composite beads. With the nanocellulose addition, the release of CEO from composite beads became slower than that of without nanocellulose. Therefore, it can be said that nanocellulose can influence the release time of antimicrobial agent from beads.

Antimicrobial test

In order to examine the antimicrobial properties of the antimicrobial sachet, *Escherichia coli*, *Aspergillus* sp, *Salmonella* sp, and *Staphylococcus aureus* were tested by Total Plate Count method. *Escherichia coli* and *Salmonella* sp are included to gram-negative bacteria, *Staphylococcus aureus* is included to gram-positive bacteria, and *Aspergillus* is included to fungi. Fig. 12 shows that antimicrobial sachet with CEO had antimicrobial activities against all the tested microorganisms. The inhibitory activities happened due to the antimicrobial activity of CEO in the produced sachet. The CEO has antibacterial activity against several pathogenic such as *Salmonella typhi*, *Salmonella paratyphi*, *Escherichia coli*, *Staphylococcus aureus*, *Pseudomonas fluorescens*, and *Bacillus licheniformis* [10].

Composite bead with 5% nanocellulose (BDNC5) had good inhibition of the microbial growth. Almost all microorganisms tested by sachet BDCN5 showed high inhibitory, 5.43% for inhibiting *Escherichia coli*, 5.19% for *Salmonella* sp, 3.36% for *Aspergillus* sp, and 8.72% for *Staphylococcus aureus*. This test supported the release characteristic test that BDNC5 had a slower release of the antimicrobial compounds so that it was able to inhibit microbial activities more effectively than others.

CONCLUSION

We successfully developed silica-alginate-nanocellulose composite beads which continuously released antimicrobial agents of cinnamon essential oil up to 6 days. Its potential use is as an antimicrobial sachet to inhibit the growth of *Escherichia coli*, *Aspergillus* sp, *Salmonella* sp, and *Staphylococcus aureus*. The addition of nanocellulose into composite beads let to slow release of CEO from composite beads and made high inhibitory of microbial activities.

ACKNOWLEDGMENTS

Financial support from Kemenristekdikti with HIKOM scheme (Contract no. 4129/IT3. L1/PN/2019) is gratefully acknowledged. The authors also would like to thank to IPB University (Bogor Agricultural University) for Program Hibah Mobilitas Dosen 2019.

CONFLICT OF INTEREST

The authors declare that there is no conflict of interests regarding the publication of this manuscript.

REFERENCES

1. Appendini P, Hotchkiss JH. Review of antimicrobial food packaging. Innovative Food Science & Emerging Technologies. 2002;3(2):113-26.
2. Ahvenainen R. Novel food packaging techniques. Woodhead Publishing Limited; 2003.
3. Otoni CG, Espitia PJP, Avena-Bustillos RJ, McHugh TH. Trends in antimicrobial food packaging systems: Emitting sachets and absorbent pads. Food Research International. 2016;83:60-73.
4.Day, B. P. F. Active Packaging of Food; Kerry, J. & Butler, P.; Eds.; Smart Packaging Technologies for Fast Moving Consumer Goods; John Wiley and Sons: New York, 2008; pp 1-18.
5. Seo H-S, Bang J, Kim H, Beuchat LR, Cho SY, Ryu J-H. Development of an antimicrobial sachet containing encapsulated allyl isothiocyanate to inactivate Escherichia coli O157:H7 on spinach leaves. International Journal of Food Microbiology. 2012;159(2):136-43.
6. Richana N, Winarti C, Hidayat T, Prastowo B. Hydrolysis of Empty Fruit Bunches of Palm Oil (Elaeis Guineensis Jacq.) by Chemical, Physical, and Enzymatic Methods for Bioethanol Production. International Journal of Chemical Engineering and Applications. 2015;6(6):422-6.
7. Fahma F, Sugiarto, Sunarti TC, Indriyani SM, Lisdayana N. Thermoplastic Cassava Starch-PVA Composite Films with Cellulose Nanofibers from Oil Palm Empty Fruit Bunches as Reinforcement Agent. International Journal of Polymer Science. 2017;2017:1-5.
8. Syverud K, Stenius P. Strength and barrier properties of MFC films. Cellulose. 2008;16(1):75-85.
9. Nair SS, Zhu JY, Deng Y, Ragauskas AJ. Hydrogels Prepared from Cross-Linked Nanofibrillated Cellulose. ACS Sustainable Chemistry & Engineering. 2014;2(4):772-80.
10. Naveed R, Hussain I, Tawab A, Tariq M, Rahman M, Hameed S, et al. Antimicrobial activity of the bioactive components of essential oils from Pakistani spices against Salmonella and other multi-drug resistant bacteria. BMC Complementary and Alternative Medicine. 2013;13(1).
11. Menggala SR, Damme PV. Improving Indonesian cinnamon (c. burmannii (Nees & t. nees) Blume) value chains for Greater Farmers Incomes. IOP Conference Series: Earth and Environmental Science. 2018;129:012026.
12. Fahma F, Iwamoto S, Hori N, Iwata T, Takemura A. Isolation, preparation, and characterization of nanofibers from oil palm empty-fruit-bunch (OPEFB). Cellulose. 2010;17(5):977-85.
13. Mishra RK, Sabu A, Tiwari SK. Materials chemistry and the futurist eco-friendly applications of nanocellulose: Status and prospect. Journal of Saudi Chemical Society. 2018;22(8):949-78.
14. Islam MT, Alam MM, Patrucco A, Montarsolo A, Zoccola M. Preparation of Nanocellulose: A Review. AATCC Journal of Research. 2014;1(5):17-23.
15. Iwamoto S, Nakagaito AN, Yano H. Nano-fibrillation of pulp fibers for the processing of transparent nanocomposites. Applied Physics A. 2007;89(2):461-6.
16. Yang H, Yan R, Chen H, Lee DH, Zheng C. Characteristics of hemicellulose, cellulose and lignin pyrolysis. Fuel.

2007;86(12-13):1781-8.
17. Łojewska J, Miśkowiec P, Łojewski T, Proniewicz LM. Cellulose oxidative and hydrolytic degradation: In situ FTIR approach. Polymer Degradation and Stability. 2005;88(3):512-20.
18. Baird MS, Hamlin JD, O'Sullivan A, Whiting A. An insight into the mechanism of the cellulose dyeing process: Molecular modelling and simulations of cellulose and its interactions with water, urea, aromatic azo-dyes and aryl ammonium compounds. Dyes and Pigments. 2008;76(2):406-16.
19. Arnata IW, Suprihatin S, Fahma F, Richana N, Candra Sunarti T. Cellulose Production from Sago Frond with Alkaline Delignification and Bleaching on Various Types of Bleach Agents. Oriental Journal of Chemistry. 2019;35(Special Issue 1):08-19.
20. Fahma F, Lisdayana N, Abidin Z, Noviana D, Sari YW, Mukti RR, et al. Nanocellulose-based fibres derived from palm oil by-products and their in vitro biocompatibility analysis. The Journal of The Textile Institute. 2019;111(9):1354-63.
21. Lisdayana N, Fahma F, Sunarti TC, Iriani ES. Thermoplastic Starch–PVA Nanocomposite Films Reinforced with Nanocellulose from Oil Palm Empty Fruit Bunches (OPEFBs): Effect of Starch Type. Journal of Natural Fibers. 2018;17(7):1069-80.
22. Pignolet LH, Waldman AS, Schechinger L, Govindarajoo G, Nowick JS, Ted L. The Alginate Demonstration: Polymers, Food Science, and Ion Exchange. Journal of Chemical Education. 1998;75(11):1430.
23.Lotfipour F, Mirzaeei S, Maghsoodi M. Evaluation of The Effect of $CaCl_2$ and Alginate Concentrations and Hardening Time on The Characteristics of *Lactobacillus Acidophilus* Loaded Alginate Beads Using Response Surface Analysis. Adv Pharm Bull, 2012; 2(1): 71-78.
24. Silverstein RM, Webster FX, Kiemle DJ. Spectrometric Identification of Organic Compounds Seventh Edition. John Wiley & Sons, Inc. New York, 2005.
25.Kalapathy U, Proctor A, Shultz JA. Simple Method for Production of Pure Silica from Rice Hull Ash. Bioresour Technol, 2000; 73 (3): 257-262.
26. Gan PG, Sam ST, Abdullah MFb, Omar MF. Thermal properties of nanocellulose-reinforced composites: A review. Journal of Applied Polymer Science. 2019;137(11):48544.
27. Rajisha KR, Deepa B, Pothan LA, Thomas S. Thermomechanical and spectroscopic characterization of natural fibre composites. Interface Engineering of Natural Fibre Composites for Maximum Performance: Elsevier; 2011. p. 241-74.
28. Borsoi C, Zimmernnam MVG, Zattera AJ, Santana RMC, Ferreira CA. Thermal degradation behavior of cellulose nanofibers and nanowhiskers. Journal of Thermal Analysis and Calorimetry. 2016;126(3):1867-78.
29. Fan X, Domszy RC, Hu N, Yang AJ, Yang J, David AE. Synthesis of silica–alginate nanoparticles and their potential application as pH-responsive drug carriers. Journal of Sol-Gel Science and Technology. 2019;91(1):11-20.
30. Johar N, Ahmad I, Dufresne A. Extraction, preparation and characterization of cellulose fibres and nanocrystals from rice husk. Industrial Crops and Products. 2012;37(1):93-9.
31. Lani NS, Ngadi N, Johari A, Jusoh M. Isolation, Characterization, and Application of Nanocellulose from Oil Palm Empty Fruit Bunch Fiber as Nanocomposites. Journal of Nanomaterials. 2014;2014:1-9.